2011

Histone modification analysis by chromatin immunoprecipitation from a low number of cells on a microfluidic platform

Tao Geng
Purdue University, tgeng@purdue.edu

Ning Bao
Virginia Tech - Blacksburg

Michael D. Litt
Ball State University

Trevor G. Glaros
Virginia Tech - Blacksburg

Liwu Li
Virginia Tech - Blacksburg

See next page for additional authors

Lab on a Chip

Cite this: *Lab Chip*, 2011, **11**, 2842

www.rsc.org/loc

PAPER

Histone modification analysis by chromatin immunoprecipitation from a low number of cells on a microfluidic platform

Tao Geng,[a] Ning Bao,[b] Michael D. Litt,[c] Trevor G. Glaros,[d] Liwu Li[d] and Chang Lu*[be]

Received 25th March 2011, Accepted 24th June 2011
DOI: 10.1039/c1lc20253g

Histone modifications are important epigenetic mechanisms involved in eukaryotic gene regulation. Chromatin immunoprecipitation (ChIP) assay serves as the primary technique to characterize the genomic locations associated with histone modifications. However, traditional tube-based ChIP assays rely on large numbers of cells as well as laborious and time-consuming procedures. Here we demonstrate a novel microfluidics-based native ChIP assay which dramatically reduces the required cell number and the assay time by conducting cell collection, lysis, chromatin fragmentation, immunoprecipitation, and washing on a microchip. Coupled with real-time PCR, our assay permits the analysis of histone modifications from as few as ~50 cells within 8.5 h. We envision that our method will provide a new approach for the analysis of epigenetic regulations and protein–DNA interactions in general, based on scarce cell samples such as those derived from animals and patients.

Introduction

Within a eukaryotic nucleus, genomic DNA is orderly organized into chromatin. The basic unit of chromatin is the nucleosome composed of 147 bp of DNA strands wrapped around a globular histone core (two H2A-H2B dimmers and a H3-H4 tetramer). The histone tails are subjected to various post-translational modifications including acetylation, methylation, phosphorylation, ubiquitination, sumoylation, deimination, isomerization and poly-ADP-ribosylation.[1,2] These modifications (also known as "the histone code") largely determine how histones interact with DNA and nonhistone proteins. Aberrant patterns in the histone code cause a variety of human diseases, ranging from different forms of cancer,[3] Huntington's disease[4] to Coffin-Lowry syndrome.[5] Among the various modifications, histone acetylation is one of the best characterized. Several lysine residues of histones H4 and H3 are acetylated, resulting in alterations to histone-DNA binding or transcription factor-chromatin interactions.[1,2]

Chromatin immunoprecipitation (ChIP) assay is the primary tool to examine histone modifications at defined genomic locations within the context of cells or tissues.[6–9] In a typical ChIP process, chromatin is released from lysed cells, digested into fragments, and selectively enriched with ChIP-grade antibodies against the protein of interest (commonly immobilized on magnetic or sepharose beads). The precipitated materials (chromatin-antibody-bead complexes) are then washed to remove the nonspecifically bound chromatin and eluted from the beads. ChIP DNA is finally purified and analyzed by PCR, sequencing or hybridization to determine the specific DNA sequence(s) associated with the protein of interest. When used for studying histone modifications, no cross-linking between the protein and the DNA sequence is necessary due to histone's high affinity to DNA.

Standard ChIP protocols, however, limit their applications to a large cell population (ideally 10^6–10^7 cells) due to sample loss after multiple steps and inefficient immunoprecipitation. This poses a serious challenge for studying epigenetic regulation networks during the processes of stem cell differentiation, embryo development and oncogenesis, because large amounts of primary cells or patient tissue biopsies are hard to harvest. In these cases, the sample amount generated by lab animals and patients is very limited. For example, the number of naturally occurring T regulatory cells in murine splenocytes is ~10,000 per spleen, and ~5000 per ml peripheral blood leukocyte. Circulating tumor cells are present at the frequency of 1–10 per ml of whole blood in patients with metastatic cancer. In addition, conventional ChIP procedures involve complex and tedious manual steps including tube-transfer, centrifugation, pipetting, and vortexing. The long assay time (typically 2–7 days) tends to cause substantial material loss, sample contamination and experimental errors. There has been substantial effort in recent years on modifying conventional ChIP protocols to allow use of small cell populations with short assay times.[10–18] Notably, a sensitivity

[a]*Birck Nanotechnology Center, Purdue University, West Lafayette, IN, 47907, USA*
[b]*Department of Chemical Engineering, Virginia Tech, Blacksburg, VA, 24061, USA. E-mail: changlu@vt.edu; Fax: +1-540-231-5022; Tel: +1-540-231-8681*
[c]*Medical Education Center, Ball State University, Muncie, IN, 47302, USA*
[d]*Department of Biological Sciences, Virginia Tech, Blacksburg, VA, 24061, USA*
[e]*School of Biomedical Engineering and Sciences, Virginia Tech-Wake Forest University, Blacksburg, VA, 24061, USA*

of ~100 cells (for examining one protein's association with multiple DNA sequences) has been demonstrated with a state-of-the-art ChIP assay.[10,14,15] Whole-genome mapping of protein–DNA interactions was conducted with 10,000 cells.[18] Some of these assays shortened the time to ~1 day. In spite of the success, most of these improved protocols still involve a significant amount of manual processing. The manual handling requires substantial labor and experience from the operator and more importantly creates a source for inconsistencies in the results due to human errors.

Microfluidics is focused on controlling and transferring tiny quantities of liquids to allow biological assays to be integrated on a small chip.[19] Microfluidic chips offer reduction in sample amounts, high level of integration and automation, and high throughput. Microfluidics provides an automated platform for performing ChIP assays based on a low number of cells with a short assay time. Although a significant amount of effort has been directed toward DNA/RNA analysis using microfluidics,[20–28] the reports on microfluidics-based ChIP assays (or studies of protein–DNA interactions) have been scarce. Wu *et al.* developed an automated microfluidic ChIP ("AutoChIP") that used 2,000 cells per reaction.[29] Oh *et al.* performed the step of immunoprecipitation on a DNA-enrichment microfluidic chip with the chromatin prepared off-chip from 2.5×10^6 cells.[30]

In this report, we demonstrate a microfluidic device that integrates all the steps involved in a ChIP assay with the exception of DNA purification and real-time PCR. We found that the microscale reaction drastically improved the assay sensitivity, and the sensitivity was also critically affected by the amount of magnetic beads used for immunoprecipitation. By optimizing the bead amount, we demonstrated microfluidic ChIP assays based on as few as ~50 cells that were finished within ~8.5 h. As a proof-of-concept, we used the microfluidic ChIP to examine histone acetylation at the chicken β-globin locus. β-globin locus is functionally important for erythropoiesis. The relationship between histone modification patterns and gene expression in the neighborhood of the chicken β-globin locus has been well-documented in previous work.[31,32] The 54 kb region is composed of the folate receptor (FR) gene at 5′ end, a ~16 kb region of condensed chromatin without genes, ~33 kb β-globin domain (containing four globin genes), and chicken odorant receptor gene at 3′ end. In 6C2 cells, an erythroid precursor cell line, the FR gene promoter is expressed and histones H3 and H4 are acetylated, whereas β-globin gene is silent and the histones are unacetylated. In this study, we confirmed the association between FR gene and acetylated histone H3 in immature 6C2 cells using the microfluidic ChIP while testing β^A-globin gene as a negative control.

Results and discussion

In this work, we describe a microfluidics-based ChIP assay with high sensitivity and rapid speed. A microfluidic chip performed integrated chromatin preparation from cells and immunoprecipitation of target protein–DNA complex in microscale channels and chambers. The microfluidic chip, as depicted in Fig. 1, has two layers of channels (separated by a thin membrane): control channels for valve actuation (55 μm deep) on the top and fluidic channels for manipulation and transport of the sample

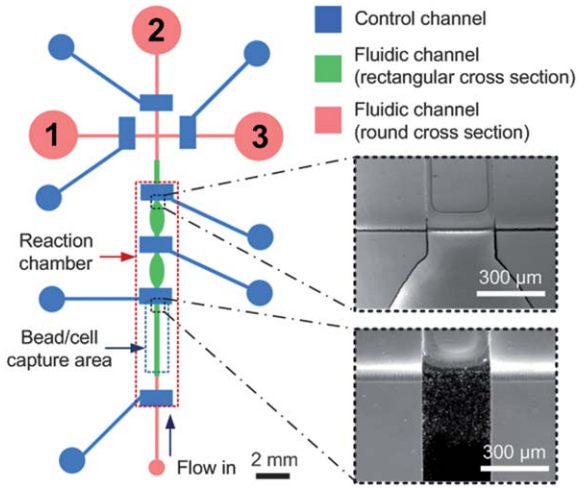

Fig. 1 The design of the integrated microfluidic chip for ChIP assay. The microfluidic chip is composed of two layers: the control layer (shown in blue) and the fluidic layer (shown in green and rose). The fluidic channel with a rectangular cross-section (shown in green) are closed partially upon actuation at the locations where it intersects with the control channel. The fluidic channel with a round cross section (shown in rose) is fully closed by the valves upon actuation. There are three reservoirs for collecting: (1) waste; (2) unbound chromatin; and (3) chromatin/bead complexes. The inset images demonstrate a partially closed valve and magnetic beads trapped by a partially closed valve.

(13 μm deep) on the bottom.[33,34] Some of the fluidic channels have rectangular cross section (300 μm wide) and are partially closed by the microfluidic valves when they are actuated, while the rest of the fluidic channels have a round cross section (200 μm wide) which are fully closed when the valves are engaged. The partially closed valves could be used to stop particle flow while permitting liquid pass through, and the fully open/closed valves allow/stop both liquid and particles. The device mainly consists of a bead/cell capture section that provides enough space for the accumulation/lysis of cells and the fragmentation of chromatin, as well as a large chamber for immunoprecipitation reaction to occur. The dimensions of each of the two elliptical chambers are 900 μm in the minor axis and 2000 μm in the major axis. The fluid and particles (cells or beads) were directed to specific locations of the chip by microfluidic valves on the chip.

As shown in Fig. 2a, 6C2 cells were first stacked against magnetic beads (functionalized with anti-acetyl histone H3 antibody). They were lysed to release chromatin (Fig. 2b) and chromatin was then sheared by micrococcal nuclease (MNase) digestion to fragments of ~200 bp (Fig. 2c). The fragmented chromatin was then incubated with the antibody-coated magnetic beads with stirring of the beads by a moving magnet and a periodically actuated valve ("flapping valve") (Fig. 2d). Once the bead surface captured acetylated histone (together with the DNA that it interacts with), the beads were washed to remove nonspecifically bound chromatin/DNA while the magnet retained the beads (Fig. 2e). The beads were then collected from an outlet of the device and taken off the chip (Fig. 2f). The DNA was eluted from the chromatin-antibody-bead by digestion with proteinase K (~1 h) and extracted by phenol-chloroform, followed by ethanol precipitation. The purification took ~3 h. The

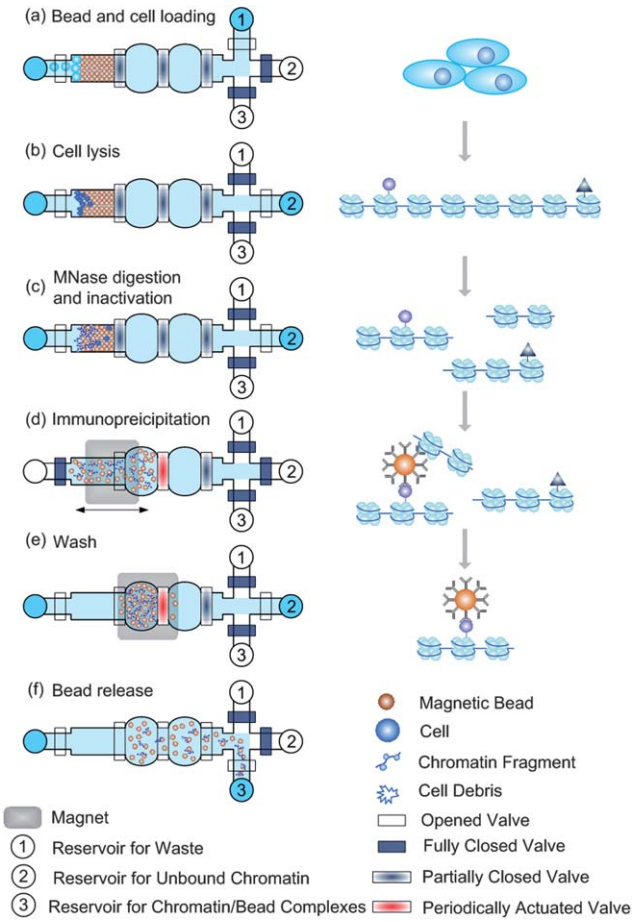

Fig. 2 The procedures involved in a microfluidic ChIP assay and the schematic of the corresponding molecular biology. **(a)** Magnetic bead and cell loading (15 min); **(b)** Cell lysis (5 min); **(c)** MNase digestion and inactivation (15 min); **(d)** Immunoprecipitation (40 min); **(e)** Wash (10 min); and **(f)** Beads release.

DNA sequence associated with the precipitated protein was then identified by real-time PCR off-chip. The device operation and the reagents involved are detailed in the experimental section below ("Microfluidic ChIP assay").

There were one inlet for infusing reagents and three outlet reservoirs (1, 2, and 3 in Fig.1 and 2) for collecting samples and waste on the microfluidic chip. The chromatin-bead complexes were recovered from 3. The solution in 1 was mostly waste buffer. 2 collected chromatin/DNA that was not bound to the bead surface (*i.e.* FR genes associated with nonacetylated histones). The solutions collected from all three reservoirs were examined by real-time PCR quantitatively in order to generate the total "input DNA" amount. The percent DNA in 3 was the "*percent precipitated DNA relative to input*" that indicates the level of a specific protein (*i.e.* acetylated histone) associated with the DNA sequence (*i.e.* FR gene). Differing from conventional ChIP assays based on $\sim 10^6$ cells, ChIP assays based on a low number of cells (10^3-10^4) also require conducting a negative control to account for the PCR signal generated by nonspecifically bound DNA, due to the accuracy required when dealing with a tiny amount of DNA.[29,35] In our experiment, we conducted the negative control by using magnetic beads without the antibody coating. When the percent precipitation (relative to the input) is significantly higher than the control, the result indicates a positive association between the protein and the DNA.

Fig. 3 shows the percent FR gene detected in reservoir 1 relative to the total amount from all three reservoirs. Samples containing 50–1000 cells were tested with functionalized beads (with anti-acetyl H3 antibody) or non-functionalized beads (as the control) used in the device. With all sample sizes, the percent DNA detected in reservoir 1 was less than 1.5%. In this case of testing ~50 cells, no DNA was detected in reservoir 1 after 40 cycles of PCR. These results indicate that there was negligible leakage of cells into the reservoir 1. 6C2 cells were efficiently captured by the packed bed of 2.8 μm magnetic beads.

Fig. 4 shows the percent DNA precipitation relative to input [calculated by [DNA3]/([DNA1]+[DNA2]+[DNA3])] obtained with beads functionalized by the antibody and beads without the antibody (the control). We used ~10 nl magnetic beads for the immunoprecipitation in these experiments. We examined two genomic locations (FR and β^A-globin genes) for enrichment of acetylated histone H3. Previous studies have shown that in 6C2 cells the FR promoter is acetylated at histone H3 and the β^A-globin promoter is unacetylated.[31,32] Fig. 4a shows that the DNA precipitation at the FR gene (black bars) increased when the cell number decreased, due to the more complete adsorption by the bead surface when there were fewer cells. The signal created by nonspecific adsorption (grey bars) was fairly constant with the changing sample size. The positive association of FR gene with acetylated H3 (indicated by the statistically significant difference between the sample signal and the background signal) was confirmed with as few as 100 cells. This is consistent with the FR gene promoter being acetylated. In comparison, there is no significant difference between the sample signal and the control

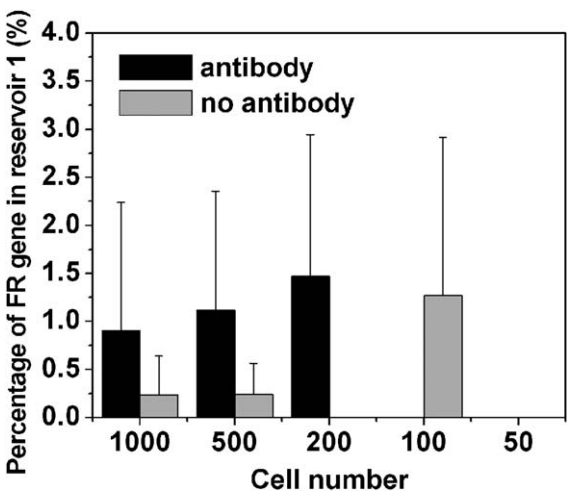

Fig. 3 The percent FR gene detected in the collection reservoir 1. 10 nl of magnetic beads coated with anti-acetyl histone H3 (black bars) or without the antibody (grey bars) were used. The percentage (Y-axis) was calculated by dividing the amount of FR gene in collection reservoir 1 by the total amount in collection reservoirs 1, 2 and 3. X-axis indicates the cell number. Each data point was generated by 3–6 independent ChIP assays (each ChIP assay was conducted on a new microchip to avoid sample contamination). All PCR measurements were run in duplicate to produce the quantification.

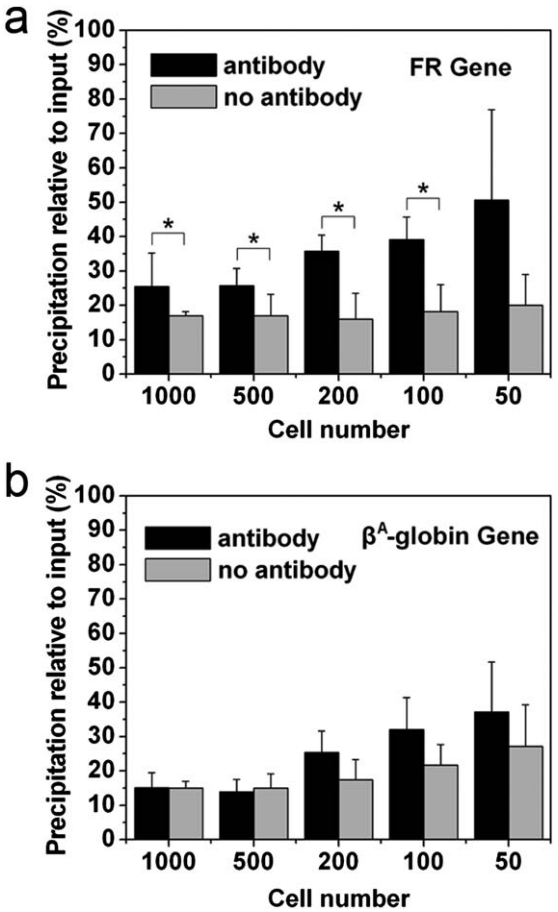

Fig. 4 The percent precipitated DNA relative to input (by microfluidic ChIP) as a function of the cell number using 10 nl of magnetic beads coated with anti-acetyl histone H3 (black bars) or without antibody (grey bars, as a control). Transcriptionally active FR gene **(a)** and silent β^A-globin gene **(b)** in 6C2 cells were analyzed. The precipitation relative to input (Y-axis) was calculated by dividing the amount of target DNA in collection reservoir 3 by the total DNA amount in collection reservoirs 1, 2 and 3. X-axis indicates the cell number. Each data point was generated by 3–6 independent ChIP assays (each ChIP assay was conducted on a new microchip to avoid sample contamination). All PCR measurements were run in duplicate to produce the quantification. * indicates statistically significant difference ($P<0.05$) calculated by unpaired two-tailed Student's *t*-test.

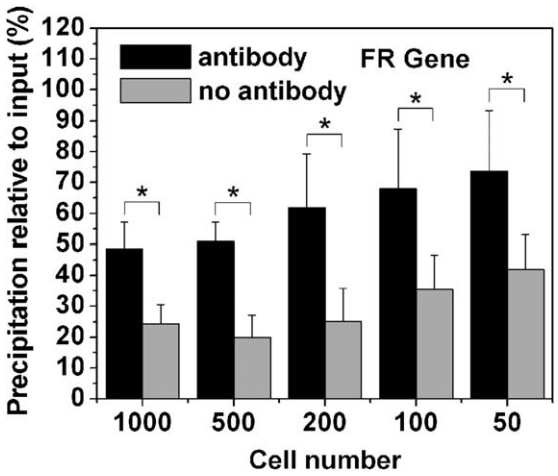

Fig. 5 The percent precipitated DNA relative to input (by microfluidic ChIP) as a function of the cell number using 20 nl of magnetic beads coated with anti-acetyl histone H3 (black bars) or without antibody (grey bars, as a control). Transcriptionally active FR gene in 6C2 cells was analyzed. The precipitation relative to input (Y-axis) was calculated by dividing the amount of target DNA in collection reservoir 3 by the total DNA amount in collection reservoirs 1, 2 and 3. X-axis indicates the cell number. Each data point was generated by 3–6 independent ChIP assays (each ChIP assay was conducted on a new microchip to avoid sample contamination). All PCR measurements were run in duplicate to produce the quantification. * indicates statistically significant difference ($P<0.05$) calculated by unpaired two-tailed Student's *t*-test.

at the β^A-globin gene promoter, indicating the absence of acetylated H3 at the β^A-globin promoter (Fig. 4b). These results agree with previous studies of histone acetylation at the FR gene and β^A-globin gene and demonstrate that our assay effectively distinguished two different levels of acetylation among two genes with different transcriptional states.

We found that the amount of magnetic beads used for the immunoprecipitation critically affected the microfluidic assay's sensitivity. In Fig. 5, we doubled the amount of beads to ~20 nl and repeated the experiments in Fig. 4. In general, we observed increased percent DNA precipitation for both the samples (black bars) and the controls (grey bars) with the higher bead loading, presumably due to the higher surface area involved for adsorption. As the net result, we were able to detect the interaction between FR gene and acetylated H3 with as few as ~50 cells. With our current device design, because increasing the bead amount seems to increase both the signal and background (created by nonspecific adsorption), there may not be benefits with increasing the bead volume further.

Several features of our device may contribute to the high sensitivity. First, the same magnetic beads were utilized to capture cells and perform immunoprecipitation and this may minimize nonspecific adsorption by the beads. Second, the chamber for cell lysis and that for immunoprecipitation are adjacent and only separated by a valve with minimal material loss during transport. Finally, our reaction chamber for immunoprecipitation is very small (~50 nl) and this may favor the collection of molecules and speed up the reaction.

Our microfluidic ChIP assay also offers the advantage of high speed. The automated on-chip procedures were finished within 1.5 h, and the entire ChIP assay was conducted within 8.5 h including off-chip protein digestion/DNA purification (~4 h) and real-time PCR (~3 h). In particular, the immunoprecipitation step was shortened to 40 min (compared to overnight in traditional ChIP protocols). A couple of factors contribute to this rapid reaction on our microfluidic chip. First, the immunoprecipitation of chromatin fragments was accelerated by incubating the antibody-coated beads with chromatins in a micrometre-sized reaction chamber (~50 nl). Such a tiny volume (compared to ~1 ml tube used in conventional assays) ensures that the concentration of chromatin was comparable to that in conventional protocols even when the number of cells is 10^4–10^5 times fewer. Second, the concentration of antibody-coated beads in the chamber was 10^2–10^3 times higher than that in conventional assays. The close proximity among beads greatly

increases the chance for chromatin adsorption on the bead surface due to short diffusion lengths involved.

Population heterogeneity may have contributed to the large standard deviations among trials seen in Fig. 4a (the 50-cell samples) and Fig. 5 (the 200, 100, and 50-cell samples). The outcome of a ChIP assay can be potentially affected when an increasingly tiny cell sample is used. For example, the global profile of histone acetylation dynamically changes as the cell cycle progresses.[36] In principle, the variations among different cell subpopulations may be amplified when the sample size approaches single cells. Consequently, ChIPs with very small cell populations has the potential to yield new insights into the heterogeneity of histone modifications and protein–DNA interactions within cell populations that is often obscured in the results of large cell population assays.

Our current assay will benefit from decreased background. We believe that the current sensitivity of the microfluidic assay can potentially be further increased by improving the washing efficiency that guarantees a complete removal of nonspecific adsorption.

Experimental

Microfluidic chip fabrication

The chip was fabricated by multilayer soft lithography technique[33,34] using polydimethylsiloxane (PDMS; RTV 615 A and B; GE Silicones, Wilton, CT, USA) as described in our previous publications.[37,38] Three photomasks were first generated with the microscale patterns designed by computer-aided design software FreeHand MX (Macromedia, San Francisco, CA, USA) and printed on high-resolution (5,080 dpi) transparencies. The master for the control layer was made of negative photoresist SU-8 2025 (Microchem, Newton, MA, USA) spun on a 3-inch silicon wafer (University Wafer, South Boston, MA, USA). The hybrid master for the fluidic layer was fabricated with negative photoresist SU-8 2010 (Microchem) and positive photoresist AZ 9260 (Clariant, Charlotte, NC, USA) on a single 3-inch silicon wafer with the channels having round and rectangular cross sections properly aligned. After development, the master was heated at 130 °C for 1 min to allow the AZ 9260 photoresist to reflow, thus yielding channels with a round cross section. Afterwards, PDMS at a mass ratio of RTV615 A: RTV615 B = 10 : 1.1 was poured onto the control layer master in a Petri dish to generate a ~ 5 mm thick control layer, and spun onto the fluidic layer master at 1100 rpm for 35 s, resulting in the thin fluidic layer (~108 μm in the thickness). Both layers of PDMS were partially cured at 80 °C for 30 min. The control layer was then peeled off from the master after cutting by a razor blade. The control layer stamp was aligned with and bonded to the fluidic layer after both PDMS surfaces were oxidized in a plasma cleaner (Harrick Plasma, Ithaca, NY, USA). The two-layer PDMS structure was baked at 80 °C for another 30 min, peeled off from the flow layer master, and punched to produce inlet and outlet reservoirs. Once the two-layer PDMS and a pre-cleaned glass slide were treated with oxygen plasma, it was immediately brought into contact against the slide to form closed channels. Finally, the assembled chip was baked at 80 °C for another 1 h to promote the bonding strength between PDMS and glass. Glass slides were cleaned in a basic solution (H_2O: 27% NH_4OH: 30% H_2O_2 = 5 : 1 : 1, volumetric ratio) at 75 °C for 3 h and then rinsed with ultrapure water and thoroughly blown dry.

System set-up and operation

The microfluidic chip was mounted on an inverted microscope (IX-71, Olympus, Melville, NY, USA) equipped with a 10× dry objective. The reagents were introduced into the inlet *via* perfluoroalkoxyalkane (PFA) high purity tubing (IDEX Health & Science, Oak Harbor, WA, USA) driven by a syringe pump (Fusion 400; Chemyx, Stafford, TX, USA). The microfluidic valves were actuated by applying a pressure in the specific control channel. The pressure deformed the thin PDMS membrane (~95 μm in the thickness) between the fluidic and control channels and closed the fluidic channel either partially or completely, depending on whether the fluidic channel cross section is rectangular or round. We used a nitrogen cylinder as the pressure source and the application/removal of the pressure was conducted *via* solenoid valves (ASCO Scientific, Florham Park, NJ, USA). A pressure regulator was used to adjust the pressure, and working pressure was typically between 30 and 40 psi. A DAQ card (NI SCB-68; National Instruments, Austin, TX, USA) and a LabVIEW (National Instruments) program were employed to control the switching of the solenoid valves. Prior to experiments, the control channels were pre-filled with water to prevent bubble formation in fluidic channels.

Magnetic bead preparation

Superparamagnetic Dynabeads® Protein A (2.8 μm, 30 mg ml^{-1}; Invitrogen, Carlsbad, CA, USA) were employed for immunoprecipitation. To reduce the nonspecific binding of chromatin, the beads were washed twice with freshly prepared and ice-cold blocking buffer [1X phosphate buffered saline (PBS; Sigma-Aldrich, St. Louis, MO, USA) containing 5 mg ml^{-1} bovine serum albumin (BSA; Sigma-Aldrich)] and resuspended in the blocking buffer. For antibody conjugation, the blocked beads were gently mixed with anti-acetyl-histone H3 antibody (final concentration 100 μg ml^{-1}; Millipore, Billerica, MA, USA), and incubated at 4 °C overnight on a rotator with a low speed. Antibody-bead complexes were then washed twice with the blocking buffer, and resuspended in the buffer to perform microfluidic ChIP assays.

Cell culture and preparation

6C2 cells were grown in α-minimal essential medium (α-MEM; Invitrogen) supplemented with 10% fetal calf serum (Invitrogen), 2% chicken serum (Invitrogen), 1 mM HEPES (pH 7.2; Sigma-Aldrich), 50 μM 2-mercaptoethanol (Pierce Biotechnology, Rockford, IL, USA) and 100 U penicillin-100 μg streptomycin/ml (Invitrogen) at 37 °C in a humidified incubator containing 5% CO_2. Cells were subcultured every two days to maintain them in exponential growth phase. Once harvested, the cells were washed twice in ice-cold PBS containing 10 mM sodium butyrate (Sigma-Aldrich) at 4 °C and resuspended in the solution with appropriate concentrations ($1-5 \times 10^5$ cells ml^{-1}, depending on the cell number used in ChIP assay). (Note: While using antibodies against acetylated histones, the presence of sodium butyrate in all

solutions is important during the whole process to inhibit the activity of deacetylase, thereby preserving the histone acetylation pattern.)

Microfluidic ChIP assay

The analysis procedure for microfluidc ChIP assay is illustrated in Fig. 2. The microchannels were initially rinsed with PBS with 0.02% Tween 20 (Sigma-Aldrich) to condition the channel and remove impurities. Subsequently, the superparamagnetic beads were loaded into the microchannels *via* the combined effects of pump-driven pressure and magnetic force generated by an external NdFeB permanent magnet (K&J Magnetics, Jamison, PA, USA). The partial closure of the valve allowed the liquid to pass through while retaining the beads. Once the beads accumulated to form a packed bed, the desired amount (1000, 500, 200, 100, or 50) of 6C2 cells were introduced into the microchannel by counting the flowing cells under a microscope. The cells were efficiently captured by the packed bed. The waste solution flowed into collection reservoir 1. The cells were then chemically lysed by infusing a small volume of lysis buffer [2% NP-40 (Sigma-Aldrich), 50 mM Tris-HCl (Sigma-Aldrich) pH 7.5, 50 mM NaCl (Sigma-Aldrich), 15 mM $MgCl_2$ (Sigma-Aldrich), 10 mM sodium butyrate, 1 mM PMSF (Sigma-Aldrich) and 1% protease inhibitor cocktail (Sigma-Aldrich); Note: the PMSF and protease inhibitor cocktail should be added freshly]. After incubation of cells in the lysis buffer for 5 min, the cell membrane was ruptured and intracellular chromatin was released. The chromatin was then sheared into small fragments by digesting with 1 U/μl MNase (Pierce Biotechnology) in the lysis buffer plus 10 mM $CaCl_2$ (Sigma-Aldrich) for 10 min. Ca^{2+} serves as an activator of the enzyme. The concentrations of both the lysis buffer and MNase on the microfluidic chip were much higher than those used in traditional ChIP assays in order to ensure rapid reactions. The enzymatic reaction was stopped by the introduction of 50 mM EDTA buffer, pH 8.0. Following the fragmentation step, all valves were closed, and a reaction chamber (as shown in Fig. 1) was formed to conduct immunoprecipitation of specific DNA-protein complex with the antibody against the acetylated histone H3 on the bead surface. The valve in between the two elliptical chambers ("periodically actuated valve") was alternating between open and closed at high frequency to disperse the packed beads in the reaction chamber and enhance mixing. A permanent magnet was also moved back and forth to generate the movement of beads and solution, thereby accelerating the antibody-antigen binding. After incubation of the chip on ice for 40 min, the bead-chromatin immunocomplexes were held in the channel with a magnet, and washed once with low salt wash buffer (10 mM Tris-HCl pH 7.4, 50 mM NaCl, 1 mM EDTA pH 8.0, 10 mM sodium butyrate, 1 mM PMSF and 1% protease inhibitor cocktail) for 5 min and once with high salt wash buffer (10 mM Tris-HCl pH 7.4, 100 mM NaCl, 1 mM EDTA pH 8.0, 10 mM sodium butyrate, 1 mM PMSF and 1% protease inhibitor cocktail) for another 5 min. In the process, the periodically actuated valve continuously worked to keep the beads loosely stacked in the solution, allowing the nonspecifically bound cellular materials and unbound chromatin fragments to be removed by the fluidic flow during the washes. The solution containing unbound chromatin flowed into collection reservoir 2. After washing, the valve was opened and the beads bound with chromatin fragments were released into collection reservoir 3.

DNA elution and purification

The samples collected from reservoirs 1, 2 and 3 were transferred to clean microcentrifuge tubes. 20 μl of the elution buffer [10 mM Tris-HCl pH 7.4, 50 mM NaCl, 10 mM EDTA pH 8.0, 0.03% sodium dodecyl sulfate (SDS; Sigma-Aldrich), 10 mM sodium butyrate, 1 mM PMSF and 1% protease inhibitor cocktail] and 0.5 μl of 20 mg ml^{-1} proteinase K (Sigma-Aldrich) were added into each sample, followed by incubating at 65 °C for 1 h. The samples were then mixed with 105 μl of 10 mM Tris-HCl buffer, pH 8.0. DNA was extracted once with phenol : chloroform : isoamyl alcohol (25 : 24 : 1; Sigma-Aldrich) and once with chloroform : isoamyl alcohol (24 : 1; Sigma-Aldrich), and then precipitated with ethanol (Sigma-Aldrich). DNA pellets were air-dried before being resuspended in 30 μl of 10 mM Tris-HCl buffer, pH 8.0.

Real-time PCR assay

The levels of DNA at target genomic sites were quantitatively measured by real-time PCR using iQ SYBR Green Supermix (Bio-Rad, Hercules, CA, USA) on an iQ5 thermocycler (Bio-Rad). All PCR assays were performed from 5 or 7.5 μl of template DNA at 95 °C for 3 min followed by 40 cycles of 95 °C for 30 s and 60 °C for 30 s. The following primers[32] specific for FR gene promoter and β^A-globin gene (IDT, Coralville, IA, USA), were used:

FR forward: 5′-AACATTACCTGCCTAGAGACTATCCA-3′

FR reverse: 5′-CTGTGTCAGAAGGCTTTCCTGTTA-3′

β^A-globin forward: 5′-CTGTGGTCTCCTGCCTCACA-3′

β^A-globin reverse: 5′-AGGCTGGGTGCCCCTC-3′

The absolute DNA concentration was calculated based on a PCR standard curve which was generated based on a serial dilution of known amounts of genomic DNA. Genomic DNA was prepared using Generation Capture Column Kit (Qiagen, Valencia, CA, USA) according to the manufacturer's instructions and dissolved in 10 mM Tris-HCl buffer, pH 8.0.

Acknowledgements

This work was supported by National Science Foundation [CBET 1016547, 0967069 to C.L.]; United States Department of Agriculture [NRI 2009-35603-05059 to C.L.]; National Institute of Health [AI64404 to L.L.]; and American Heart Association grant [to L.L.].

References

1 T. Kouzarides, *Cell*, 2007, **128**, 693–705.
2 T. Jenuwein and C. D. Allis, *Science*, 2001, **293**, 1074–1080.
3 M. Esteller, *Nat. Rev. Genet.*, 2007, **8**, 286–298.
4 G. Sadri-Vakili and J. H. Cha, *Nat. Clin. Pract. Neurol.*, 2006, **2**, 330–338.
5 J. Ausio, D. B. Levin, G. V. De Amorim, S. Bakker and P. M. Macleod, *Clin. Genet.*, 2003, **64**, 83–95.
6 V. A. Spencer, J. M. Sun, L. Li and J. R. Davie, *Methods*, 2003, **31**, 67–75.

7 B. E. Bernstein, E. L. Humphrey, C. L. Liu and S. L. Schreiber, *Methods Enzymol.*, 2004, **376**, 349–360.
8 D. J. Clark and C. H. Shen, *Methods Enzymol.*, 2006, **410**, 416–430.
9 P. Dasgupta and S. P. Chellappan, *Methods Mol. Biol.*, 2007, **383**, 135–152.
10 L. P. O'Neill, M. D. VerMilyea and B. M. Turner, *Nat. Genet.*, 2006, **38**, 835–841.
11 J. A. Dahl and P. Collas, *Stem Cells*, 2007, **25**, 1037–1046.
12 L. G. Acevedo, A. L. Iniguez, H. L. Holster, X. Zhang, R. Green and P. J. Farnham, *BioTechniques*, 2007, **43**, 791–797.
13 J. L. Attema, P. Papathanasiou, E. C. Forsberg, J. Xu, S. T. Smale and I. L. Weissman, *Proc. Natl. Acad. Sci. U. S. A.*, 2007, **104**, 12371–12376.
14 J. A. Dahl and P. Collas, *Nat. Protoc.*, 2008, **3**, 1032–1045.
15 J. A. Dahl and P. Collas, *Nucleic Acids Res.*, 2008, **36**, e15.
16 J. A. Dahl, A. H. Reiner and P. Collas, *GenomeBiology*, 2009, **10**, R13.
17 M. L. Sikes, J. M. Bradshaw, W. T. Ivory, J. L. Lunsford, R. E. McMillan and C. R. Morrison, *J. Immunol. Methods*, 2009, **344**, 58–63.
18 M. Adli, J. Zhu and B. E. Bernstein, *Nat. Methods*, 2010, **7**, 615–618.
19 P. Mitchell, *Nat. Biotechnol.*, 2001, **19**, 717–721.
20 M. A. Burns, B. N. Johnson, S. N. Brahmasandra, K. Handique, J. R. Webster, M. Krishnan, T. S. Sammarco, P. M. Man, D. Jones, D. Heldsinger, C. H. Mastrangelo and D. T. Burke, *Science*, 1998, **282**, 484–487.
21 J. W. Hong, V. Studer, G. Hang, W. F. Anderson and S. R. Quake, *Nat. Biotechnol.*, 2004, **22**, 435–439.
22 R. Pal, M. Yang, R. Lin, B. N. Johnson, N. Srivastava, S. Z. Razzacki, K. J. Chomistek, D. C. Heldsinger, R. M. Haque, V. M. Ugaz, P. K. Thwar, Z. Chen, K. Alfano, M. B. Yim, M. Krishnan, A. O. Fuller, R. G. Larson, D. T. Burke and M. A. Burns, *Lab Chip*, 2005, **5**, 1024–1032.
23 M. A. Witek, S. D. Llopis, A. Wheatley, R. L. McCarley and S. A. Soper, *Nucleic Acids Res.*, 2006, **34**, e74.
24 S. W. Yeung, T. M. H. Lee, H. Cai and I. M. Hsing, *Nucleic Acids Res.*, 2006, **34**, e118.
25 N. Agrawal, Y. A. Hassan and V. M. Ugaz, *Angew. Chem., Int. Ed.*, 2007, **46**, 4316–4319.
26 B. R. Cipriany, R. Zhao, P. J. Murphy, S. L. Levy, C. P. Tan, H. G. Craighead and P. D. Soloway, *Anal. Chem.*, 2010, **82**, 2480–2487.
27 K. A. Hagan, C. R. Reedy, M. L. Uchimoto, D. Basu, D. A. Engel and J. P. Landers, *Lab Chip*, 2011, **11**, 957–961.
28 R. Novak, Y. Zeng, J. Shuga, G. Venugopalan, D. A. Fletcher, M. T. Smith and R. A. Mathies, *Angew. Chem., Int. Ed.*, 2011, **50**, 390–395.
29 A. R. Wu, J. B. Hiatt, R. Lu, J. L. Attema, N. A. Lobo, I. L. Weissman, M. F. Clarke and S. R. Quake, *Lab Chip*, 2009, **9**, 1365–1370.
30 H. J. Oh, J. Y. Park, S. E. Park, B. Y. Lee, J. S. Park, S. K. Kim, T. J. Yoon and S. H. Lee, *Anal. Chem.*, 2009, **81**, 2832–2839.
31 M. D. Litt, M. Simpson, M. Gaszner, C. D. Allis and G. Felsenfeld, *Science*, 2001, **293**, 2453–2455.
32 M. D. Litt, M. Simpson, F. Recillas-Targa, M. N. Prioleau and G. Felsenfeld, *EMBO J.*, 2001, **20**, 2224–2235.
33 M. A. Unger, H. P. Chou, T. Thorsen, A. Scherer and S. R. Quake, *Science*, 2000, **288**, 113–116.
34 T. Thorsen, S. J. Maerkl and S. R. Quake, *Science*, 2002, **298**, 580–584.
35 J. D. Nelson, O. Denisenko and K. Bomsztyk, *Nat. Protoc.*, 2006, **1**, 179–185.
36 K. J. McManus and M. J. Hendzel, *Biochem. Cell Biol.*, 2006, **84**, 640–657.
37 J. Wang, M. J. Stine and C. Lu, *Anal. Chem.*, 2007, **79**, 9584–9587.
38 H. Y. Wang, N. Bao and C. Lu, *Biosens. Bioelectron.*, 2008, **24**, 613–617.

